

IMPROVED RECONSTRUCTION OF IMAGES DISTORTED BY WATER WAVES

Arturo Donate and Eraldo Ribeiro
Department of Computer Sciences
Florida Institute of Technology
Melbourne, FL 32901

Keywords: Image recovery, reconstruction, distortion, refraction, motion blur, water waves, frequency domain.

Abstract: This paper describes a new method for removing geometric distortion in images of submerged objects observed from outside shallow water. We focus on the problem of analyzing video sequences when the water surface is disturbed by waves. The water waves will affect the appearance of the individual video frames such that no single frame is completely free of geometric distortion. This suggests that, in principle, it is possible to perform a selection of a set of low distortion sub-regions from each video frame and combine them to form a single undistorted image of the observed object. The novel contribution in this paper is to use a multi-stage clustering algorithm combined with frequency domain measurements that allow us to select the best set of undistorted sub-regions of each frame in the video sequence. We evaluate the new algorithm on video sequences created both in our laboratory, as well as in natural environments. Results show that our algorithm is effective in removing distortion caused by water motion.

1 INTRODUCTION

In this paper, we focus on the problem of recovering a single undistorted image from a set of non-linearly distorted images. More specifically, we are interested in the case where an object submerged in water is observed by a video camera from a static viewpoint above the water. The water surface is assumed to be disturbed by waves. Figure 1 shows a sample of frames from a video of a submerged object viewed from above. This is an interesting and difficult problem mainly when the geometry of the scene is unknown. The overall level of distortion in each frame depends on three main parameters of the wave model: the amplitude, the speed of oscillation, and the slope of the local normal vector on the water surface. The amplitude and slope of the surface normal affect the refraction of the viewing rays causing geometric distortions while the speed of oscillation causes motion blur due to limited video frame rate.

Our goal in this paper is to recover an undistorted image of the underwater object given only a video of the object as input. Additionally, no previous knowledge of the waves or the underwater object is assumed. We propose to model the geometric distortions and the motion blur separately from each other.

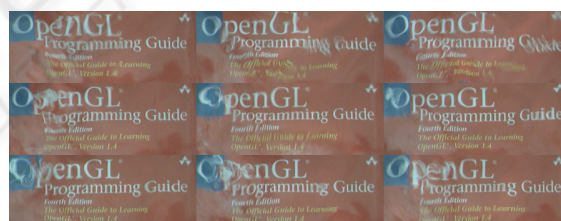


Figure 1: An arbitrary selection of frames from our low energy wave data set.

We analyse geometric distortions via clustering, while measuring the amount of motion blur by analysis in the frequency domain in an attempt to separate high and low distortion regions. Once these regions are acquired, we combine single samples of neighboring low distortion regions to form a single image that best represents the object.

We test our method on different data sets created both in the laboratory as well as outdoors. Each experiment has waves of different amplitudes and speeds, in order to better illustrate its robustness. Our current experiments show very promising results.

The remainder of the paper is organized as follows. We present a review of the literature in Section 2. In

Section 3, we describe the geometry of refraction distortion due to surface waves. Section 4 describes the details of our method. In Section 5, we demonstrate our algorithm on video sequences acquired in the laboratory and outdoors. Finally, in Section 6, we present our conclusions and directions for future work.

2 RELATED WORK

Several authors have attempted to approach the general problem of analyzing images distorted by water waves. The dynamic nature of the problem requires the use of video sequences of the target scene as a primary source of information. In the discussion and analysis that follow in this paper, we assume that frames from an acquired video are available.

The literature has contributions by researchers in various fields including computer graphics, computer vision, and ocean engineering. Computer graphics researchers have primarily focused on the problem of rendering and reconstructing the surface of the water (Gamito and Musgrave, 2002; Premoze and Ashikhmin, 2001). Ocean engineering researchers have studied sea surface statistics and light refraction (Walker, 1994) as well as numerical modeling of surface waves (Young, 1999). The vision community has attempted to study light refraction between water and materials (Mall and da Vitoria Lobo, 1995), recover water surface geometry (Murase, 1992), as well as reconstruct images of submerged objects (Efros et al., 2004; Shefer et al., 2001). In this paper, we focus on the problem of recovering images with minimum distortion.

A simple approach to the reconstruction of images of submerged objects is to perform a temporal average of a large number of continuous video frames acquired over an extended time duration (i.e., mean value of each pixel over time) (Shefer et al., 2001). This technique is based on the assumption that the integral of the periodic function modeling the water waves is zero (or constant) when time tends to infinity. Average-based methods such as the one described in (Shefer et al., 2001) can produce reasonable results when the distortion is caused by low energy waves (i.e., waves of low amplitude and low frequency). However, this method does not work well when the waves are of higher energy, as averaging over all frames equally combines information from both high and low distortion data. As a result, the averaged image will appear blurry and the finer details will be lost.

Modeling the three-dimensional structure of the waves also provides a way to solve the image recovery problem. Murase (Murase, 1992) approaches the problem by first reconstructing the 3D geometry of

the waves from videos using optical flow estimation. He then uses the estimated optical flow field to calculate the water surface normals over time. Once the surface normals are known, both the 3D wave geometry and the image of submerged objects are reconstructed. Murase's algorithm assumes that the water depth is known, and the amplitude of the waves is low enough that there is no separation or elimination of features in the image frames. If these conditions are not met, the resulting reconstruction will contain errors mainly due to incorrect optical flow extraction.

More recently, Efros et al. (Efros et al., 2004) proposed a graph-based method that attempts to recover images with minimum distortion from videos of submerged objects. The main assumption is that the underlying distribution of local image distortion due to refraction is Gaussian shaped (Cox and Munk, 1956). Efros et al., propose to form an embedding of subregions observed at a specific location over time and then estimate the subregion that corresponds to the center of the embedding. The Gaussian distortion assumption implies that the local patch that is closer to the mean is fronto-parallel to the camera and, as a result, the underwater object should be clearly observable through the water at that point in time. The solution is given by selecting the local patches that are the closest to the center of their embedding. Efros et al., propose the use of a shortest path algorithm that selects the solution as the frame having the shortest overall path to all the other frames. Distances were computed transitively using normalized cross-correlation (NCC). Their method addresses likely leakage problems caused by erroneous shortest-distances between similar but blurred patches by calculating paths using a convex flow approach. The sharpness of the image reconstruction achieved by their algorithm is very high compared to average-based methods even when applied to sequences distorted by high energy waves.

In this paper we follow Efros et al. (Efros et al., 2004), considering an ensemble of fixed local regions over the whole video sequence. However, our method differs from theirs in two main ways. First, we propose to reduce the leakage problem by addressing the motion blur effect and the refraction effect separately. Second, we take a frequency domain approach to the problem by quantifying the amount of motion blur present in the local image regions based on measurements of the total energy in high frequencies.

Our method aims at improving upon the basic average-based techniques by attempting to separate image subregions into high and low distortion groups. The K-Means algorithm (Duda et al., 2000) is used along with a frequency domain analysis for generating and distinguishing the two groups in terms of the quality of their member frames. Normalized cross-correlation is then used as a distance measurement to

find the single frame that best represents the undistorted view of the region being analyzed.

3 DISTORTION ANALYSIS

In the problem considered in this paper, the local image distortions caused by random surface waves can be assumed to be modeled by a Gaussian distribution (Efros et al., 2004; Cox and Munk, 1956). The magnitude of the distortion at a given image point increases radially, forming a disk in which the center point contains the least amount of distortion. The center subregion can be determined by a clustering algorithm if the distribution of the local patches is not too broad (i.e., the diameter of the disk is small) (Efros et al., 2004). Our method effectively reduces the size of this distortion embedding by removing the subregions containing large amounts of translation and motion blur. In this section, we analyze how refraction and motion blur interferes with the appearance of submerged objects observed from outside the water. First, we analyze the geometry of refraction and its relationship to both the surface normals of the waves and the distance from the camera to the water. We then analyze the motion blur distortion caused by the speed of oscillation of the waves, and how it can be quantified in the frequency domain.

3.1 Refraction Caused by Waves

Consider a planar object submerged in shallow transparent water. The object is observed from a static viewpoint above the water by a video camera with optical axis perpendicular to the submerged planar object. In our modeling, we assume that only the water is moving in the scene (i.e., both the camera and the underwater object are stationary). Additionally, the depth of the object is assumed to be unknown and constant. Figure 2 illustrates the geometry of the scene. In the figure, d is the distance between the camera and a point where the ray of light intersects the water surface (i.e., point of refraction). The angle between the viewing ray and the surface normal is θ_n , and the angle between the refracted viewing ray and the surface normal is θ_r . These two angles are related by Snell's law (1). The camera c observes a submerged point p . The angle α measures the relative translation of the point p when the viewing ray is refracted by the water waves.

According to the diagram in Figure 2, the image seen by the camera is distorted by refraction as a function of both the angle of the water surface normal at the point of refraction and the amplitude of the water waves. If the water is perfectly flat (i.e., there are no waves), there will be no distortion due to refraction.

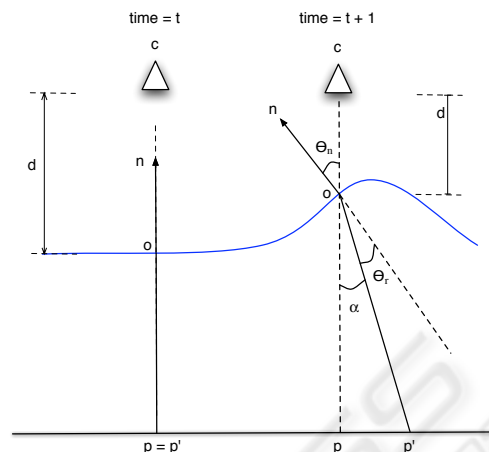


Figure 2: Geometry of refraction on a surface disturbed by waves. The camera c observes a given point p on the submerged planar object. The slant angle of the surface normal (θ_n) and the distance from surface to the camera (d) are the main parameters of our distortion model. When θ_n is zero, the camera observes the point p at its original location on the object (i.e., there is no distortion in the image). If θ_n changes, the apparent position of p changes by a translation factor with magnitude $\|p' - p\|$. This magnitude also varies as a function of the distance from the water surface to the camera (e.g., due to the amplitude of the waves). The figure also illustrates the light refracting with the waves at two different points in time. The image at time t would appear clear while the image at time $t+1$ would be distorted by refraction.

However, if the surface of the water is being disturbed by waves, the nature of the image distortion becomes considerably more complex. In this paper, we will focus on the case where the imaged object is planar and is parallel to the viewing plane (i.e., the planar object is perpendicular to the optical axis of the camera).

In the experiments described in this paper, the main parameters that model the spatial distortion in the image are the slant angle of the surface normal (θ_n) and the distance from surface to the camera (d). The two parameters affect the image appearance by translating image pixels within a small local neighborhood. More specifically, the varying slope of the waves and their amplitude will modify the angle of refraction that will result in the distortion of the final image. Additionally, considerable motion blur can occur in each video frame due to both the limited capture frequency of the video system, and the dynamic nature of the liquid surface. The blur will have different magnitudes across the image in each video frame. In our experiments, varying levels of motion blur will be present in each frame depending on the speed of change in the slant of the surface normals. Next, we show that the translation caused by refraction is linear with respect

to the distance d and non-linear with respect to the slant angle of the water surface normal (θ_n).

We commence by modeling the refraction of the viewing ray. The refraction of light from air to water is given by Snell's law as:

$$\sin \theta_n = r_w \sin \theta_r \quad (1)$$

where θ_n is the angle of incidence of light. In our case, θ_n corresponds to the slant angle of the water surface normal. θ_r is the angle of refraction between the surface normal and the refracted viewing ray. The air refraction coefficient is assumed to be the unit and r_w is the water refraction coefficient ($r_w = 1.33$). From Figure 2, the angle that measures the amount of translation when θ_n varies is given by:

$$\alpha = \theta_n - \theta_r \quad (2)$$

Solving for θ_r in Equation 1 and substituting the result into Equation 2 we have:

$$\alpha = \theta_n - \arcsin\left(\frac{\sin \theta_n}{r_w}\right) \quad (3)$$

Considering the triangle $\Delta \mathbf{opp}'$, the magnitude of the underwater translation is given by:

$$\|\mathbf{p}_i - \mathbf{p}\| = d \tan \alpha \quad (4)$$

From (3), the overall translation is:

$$\|\mathbf{p}_i - \mathbf{p}\| = d \tan\left[\theta_n - \arcsin\left(\frac{\sin \theta_n}{r_w}\right)\right] \quad (5)$$

Equation 5 describes the translational distortion of underwater points caused by two parameters: the slant angle of the surface normal and the distance between the camera and the point of refraction. The magnitude of translation in (5) is linear with respect to d and non-linear with respect to θ_n . These two variables will vary according to the movement of the water waves. For a single sinusoidal wave pattern model, the amplitude of the wave will affect d while the slope of the waves will affect the value of θ_n . The distortion modeled by Equation 5 vanishes when $d = 0$ (i.e., the camera is underwater), or the angle θ_n is zero (i.e., the surface normal is aligned with the viewing direction).

3.2 Motion Blur and Frequency Domain

Motion blur accounts for a large part of the distortion in videos of submerged objects when the waves are of high energy. The speed of oscillation of the surface waves causes motion blur in each frame due to limited video frame rate. Studies have shown that an increase in the amount of image blur decreases the total high frequency energy in the image (Field and Brady, 1997).

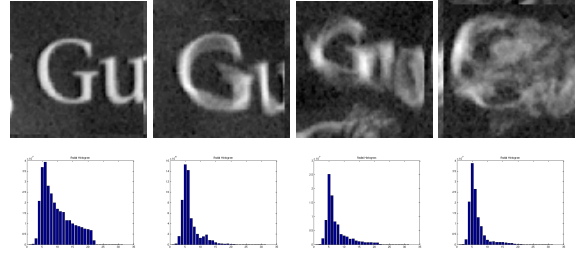


Figure 3: Blur and its effect on the Fourier domain. Top row: images with increasing levels of blur. Bottom row: corresponding radial frequency histograms. Blur causes a fast drop in energy in the radial spectral descriptor (decrease in high frequency content).

Figure 3 shows some examples of regions with motion blur distortion (top row) and their corresponding radial frequency histograms after a high-pass filter is applied to the power spectrum (bottom row). The decrease of energy in high frequencies suggests that, in principle, it is possible to determine the level of blur in images of the same object by measuring the total energy in high frequencies.

As pointed out in (Field and Brady, 1997), measuring the decay of high-frequency energy alone does not work well for quantifying motion blur of different types of images, as a simple reduction of the total number of edges in an image will produce power spectra with less energy in higher frequencies but no decrease in the actual image sharpness. Alternatively, blur in images from different scenes can be more effectively quantified using measures such as the phase coherence described in (Wang and Simoncelli, 2004).

In this paper, we follow (Field and Brady, 1997) by using a frequency domain approach to quantify the amount of motion blur in an image. We use the total energy of high-frequencies as a measure of image quality. This measurement is able to accurately quantify relative blur when images are taken from the same object or scene (e.g., images roughly containing the same number of edges).

In order to detect the amount of blur present in a set of images corresponding to the same region of the object, we first apply a high-pass filter to the power spectrum of each image. We express the filtered power spectrum in polar coordinates to produce a function $S(r, \theta)$, where S is the spectrum function, r and θ are the variables in this coordinate system. A global description of the spectral energy can be obtained by integrating the the polar power spectrum function into 1D histograms as follows (Gonzalez and Woods, 1992):

$$S(r) = \sum_{\theta=0}^{\pi} S(r, \theta) \quad (6)$$

Summing the high-frequency spectral energy in the 1D histograms provides us with a simple way to determine changes in the level of blur when comparing blurred versions of the same image. Figure 3 (bottom row) shows a sample of radial frequency histograms. The low frequency content in the histograms has been filtered out by the high-pass filter. The decrease in the high-frequency energy corresponds to an increase on the level of motion blur in the images.

4 METHOD OVERVIEW

Let us assume that we have a video sequence with N frames of a submerged object. We commence by sub-dividing all the video frames into K small overlapping sub-regions ($R_k = \{\mathbf{x}_1, \dots, \mathbf{x}_N\}$, $k = 1, \dots, K$). The input data of our algorithm consists of these K sets of smaller videos describing the local refraction distortion caused by waves on the actual large image. The key assumption here is that local regions will sometimes appear undistorted as the surface normal of the local plane that contains the region is aligned with the optical axis of the camera. Our goal is to determine the local region frame inside each region dataset that is closest to that fronto-parallel plane. We approach the problem by assuming that there will be two main types of distortion in the local dataset. The distortions are described in Section 3. The first type is the one caused by pure refraction driven by changes in both distance from the camera to the water and the angle of the water surface normal. The second type of distortion is the motion blur due to the speed of oscillation of the waves. Refraction and blur affect the local appearance of the frames in distinct ways. The first causes the local regions to translate across neighboring sub-regions while the second causes edges to become blurred. The exact interplay between these two distortions is complex. The idea in our algorithm is to quantify these distortions and select a reduced set of high-quality images from which we will choose the best representative region frames.

We start by clustering each local dataset into groups with the K-Means algorithm (Duda et al., 2000), using the Euclidean distance between the frames as a similarity measure. Since no previous knowledge of the scene is available, the K-Means centers were initialized with a random selection of sample subregions from the dataset. The clustering procedure mainly separates the frames distorted by translation. We expect the frames with less translation distortion to cluster together. However, some of the resulting clusters will contain frames with motion blur. In our experiments, the Euclidean distance measurement has shown good results in grouping most, if not all, of the

Algorithm 1 Multi-stage clustering.

Given N video frames:

- 1: Divide frames into K overlapping sub-regions.
 - 2: Cluster each set of sub-regions to group the low distortion frames.
 - 3: Remove the images with high level of blur from each group of low distortion frames.
 - 4: Select the closest region to all other regions in that set using cross-correlation.
 - 5: Create a final reconstructed single large image by mosaicking all subregions.
 - 6: Apply a blending technique to reduce tiling artifacts between neighboring regions.
-

lower distortion frames together, with some high distortion frames present. The initial number of clusters is very important. We found that the more clusters we could successfully split a data set into, the easier it was for the rest of the algorithm to obtain a good answer. To guarantee convergence, re-clustering was performed when one of the clusters had less than 10% of the total number of frames (e.g., in an 80-frame data set, each of the four clusters must have at least eight frames or we re-cluster the data). The algorithm initially attempts to divide the data into 10 clusters. If each cluster does not contain at least 10% of the total number of frames after a certain number of iterations, we reduce the number of clusters by one and repeat the process until the data is successfully clustered.

We assume that one of the resulting clusters produced by the K-Means algorithm contains mostly low distortion frames. To distinguish it from the other clusters, we take a statistical approach by assuming that the cluster containing most of the low distortion frames has the least amount of pixel change across frames. This is equivalent to saying that the frames should be similar in appearance to each other. We compute the variance of each pixel over all frames in the cluster using

$$\sigma^2 = \frac{1}{n} \sum_{i=1}^n (p_i - \bar{p})^2 \quad (7)$$

where n is the number of frames in the cluster, p_i is the pixel value of the i -th image frame for that point, and \bar{p} is the mean pixel value for that point over all frames in the cluster. We take the sum of the variances of all the pixels for each cluster, and the cluster with the minimum total variance is labeled as the low distortion group. Our experiments show that this technique is approximately 95% successful in distinguishing the best cluster. The algorithm discards all frames that are not in the cluster with the lowest total variance.

At this point, we have greatly reduced the number of frames for each region. The next step of the algorithm is to rank all frames in this reduced dataset

with respect to their sharpness. As described in Section 3, the Fourier spectrum of frames containing motion blur tend to present low energy in high frequency. This allows us to remove the frames with high level of blur by measuring the decay of high frequency energy in the Fourier domain. We calculate the mean energy of all frame regions and discard the ones whose energy is less than the mean.

Finally, the algorithm produces a subset of frame regions which are similar in appearance to each other and have small amounts of motion blur. We then choose a single frame from this set to represent the fronto-parallel region. In (Efros et al., 2004), this was done using a graph theory approach by running a shortest path algorithm. We take a somewhat similar approach, computing the distances between all the frames via normalized cross-correlation then finding the frame whose distance is the closest to all the others. This is equivalent to finding the frame closest to the mean of this reduced set of frames. We then mosaic all sub-regions and use a blending algorithm (Szeliski and Shum, 1997) to produce the final reconstructed image.

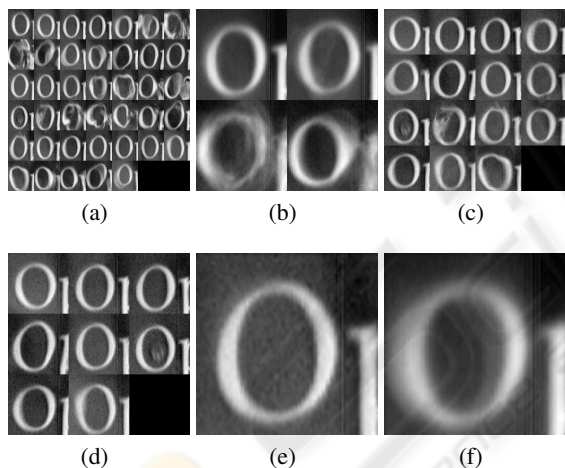


Figure 4: (a) Subregions being compared. (b) Mean of the 4 resulting clusters, (c) frames belonging to the chosen sharpest cluster, (d) frames remaining after removing those with lower high frequency values, (e) final frame choice to represent subregion, (f) and average over all frames (shown for comparison).

Figure 4 illustrates the steps for finding the best frame of each set. The algorithm takes the frames in each subregion (Figure 4a) and use K-Means to produce four clusters (Figure 4b). After variance calculations, the algorithm determined the top-left cluster of Figure 4b to be the one with the least overall distortion. The images in this cluster are then ranked in decreasing order of high-frequency energy and those frames whose energy is lower than the mean are re-

moved in an attempt to further reduce the dataset. The remaining frames are shown in Figure 4d. From this reduced set, normalized cross correlation distances are computed in an attempt to find the best choice. Figure 4e shows the output, and Figure 4f shows the temporal average of the region for comparison.

5 EXPERIMENTS

In this section we present experimental results for video sequences recorded in the laboratory and in natural environments. Current experiments show very promising results.

In the first experiment, we analyze an 80-frame video sequence (Figure 1). The waves in this data set were low energy waves, large enough to cause a considerable amount of distortion, yet small enough not to cause any significant separation or occlusion of the submerged object. The level of distortion in this dataset is similar to the one used in (Murase, 1992). Our method provides much sharper results when compared to simple temporal averaging. We extracted the subregions with 50% overlap. A simple blending process (Szeliski and Shum, 1997) is applied to reduce the appearance of “tiles” as observed in the final reconstructed image. The results can be seen in Figure 5. As expected, the blending process slightly reduced the sharpness of the image in some cases due to the fact that it is a weighted averaging function.

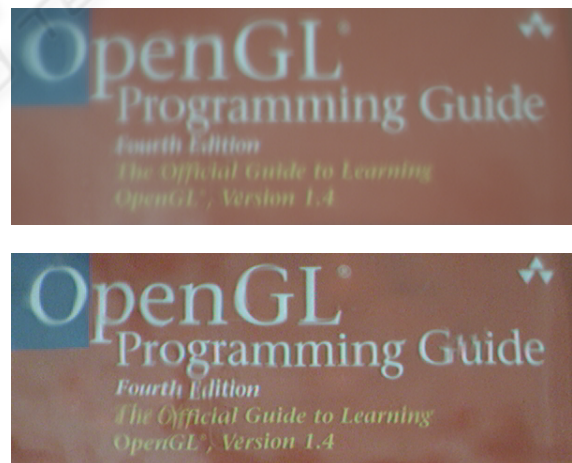


Figure 5: Low-energy wave dataset. (a) Average over all frames. (b) Output using our method.

The next experiment shows the output of the algorithm when the input video sequence contains waves of high energy. These waves may occlude or separate the underwater object at times, temporarily making subregions completely blurry and unrecognizable.

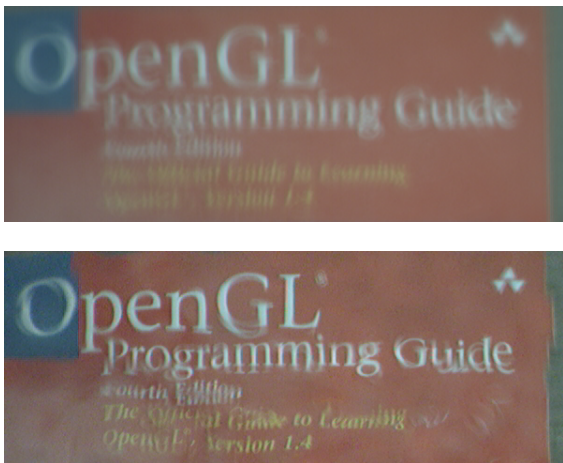


Figure 6: High-energy wave dataset. (a) Average over all frames. (b) Output using our method.

For a few regions of the image, the dataset does not contain a single frame in which the object is clearly observed, making it difficult to choose a good frame from the set. The blur and occlusion complicate the reconstruction problem, but our algorithm handles it well by explicitly measuring blur and using it to select high-quality frames from each cluster. Figure 6 shows our results.

Our final experiments deal with datasets obtained in a natural outdoor environment. The videos were acquired from the moving stream of a small creek. The waves in this dataset are of high energy, but unlike the previous dataset, these are of low magnitude but very high frequency and speed, naturally generated by the creek's stream. Figures 7 and 8 show our results.

6 CONCLUSIONS

We propose a new method for recovering images of underwater objects distorted by surface waves. Our method provides promising improved results over computing a simple temporal average. It begins by dividing the video frames into subregions followed by a temporal comparison of each region, filtering out the low distortion frames via the K-Means algorithm and frequency domain analysis of motion blur.

In our method, we approach the problem in a way similar to (Efros et al., 2004) as we perform a temporal comparison of subregions to estimate the center of the Gaussian-like distribution of an ensemble of local subregions. Our approach differs from theirs in two main aspects. First, we considerably reduce the “leakage” problem (i.e., erroneous NCC correlations being



Figure 7: Creek stream data set 1. (a) Average over all frames. (b) Output using our method.

classified as shortest distances) by clustering the subregions using a multi-stage approach that reduces the data to a small number of high-quality regions. Second, we use frequency-domain analysis that allows us to quantify the level of distortion caused by motion blur in the local sub-regions. Our results show that the proposed method is effective in removing distortion caused by refraction in situations when the surface of the water is being disturbed by waves. A direct comparison between our method and previously published methods (Efros et al., 2004; Murase, 1992; Shefer et al., 2001) is difficult due to the varying wave conditions between data sets, as well as the lack of a method for quantifying the accuracy of the reconstruction results.

Working with video sequences that contain high energy waves is a complex task due to occlusion and blurriness introduced into the image frames. Our algorithm handles these conditions well by explicitly measuring blur in each subregion. Additionally, large energy waves introduce the problem that a given embedding of subregions may not contain a single frame corresponding, or near, to a point in time when the

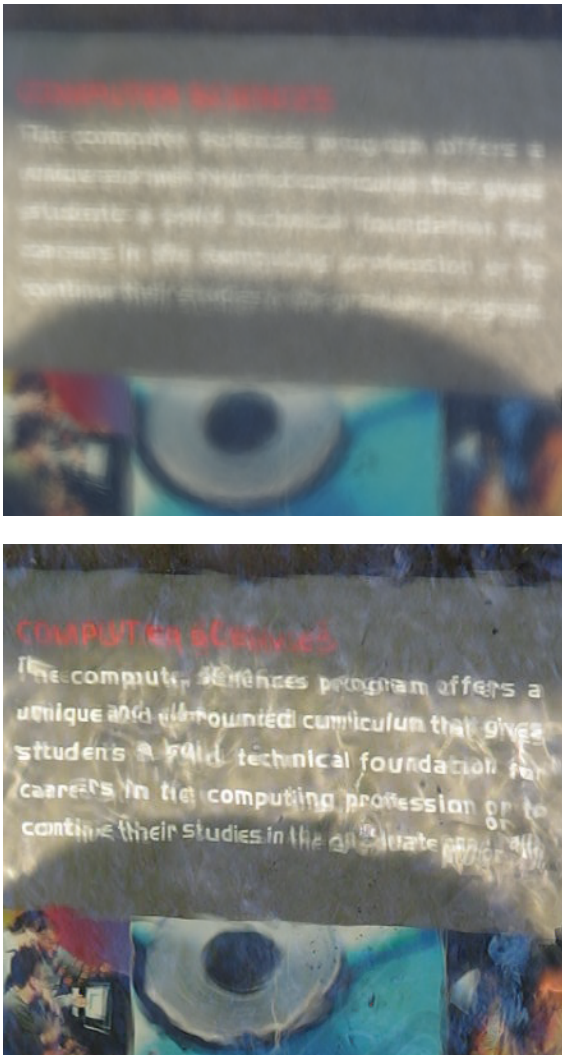


Figure 8: Creek stream data set 2. (a) Average over all frames. (b) Output using our method.

water normal is parallel to the camera's optical axis. This affects the quality of our results.

Our plans for future research involve extending the current algorithm to improve results when dealing with high energy waves. We are currently researching the incorporation of constraints provided by neighboring patches. These constraints can, in principle, be added by means of global alignment algorithms. Further lines of research involve extending the current method to use explicit models of both waves and refraction in shallow water (Gamito and Musgrave, 2002), and the application of our ideas to the problem of recognizing submerged objects and textures. We are currently working on developing these ideas and they will be reported in due course.

ACKNOWLEDGMENTS

The authors would like to thank Dr. Alexey Efros for kindly providing us with an underwater video sequence which we used to initially develop and test our algorithm.

REFERENCES

- Cox, C. and Munk, W. (1956). Slopes of the sea surface deduced from photographs of the sun glitter. *Bull. Scripps Inst. Oceanogr.*, 6:401–488.
- Duda, R. O., Hart, P. E., and Stork, D. G. (2000). *Pattern Classification (2nd Edition)*. Wiley-Interscience.
- Efros, A., Isler, V., Shi, J., and Visontai, M. (2004). Seeing through water. In Saul, L. K., Weiss, Y., and Bottou, L., editors, *Advances in Neural Information Processing Systems 17*, pages 393–400. MIT Press, Cambridge, MA.
- Field, D. and Brady, N. (1997). Visual sensitivity, blur and the sources of variability in the amplitude spectra of natural scenes. *Vision Research*, Dec;37(23):3367–83, 37(23):3367–3383.
- Gamito, M. N. and Musgrave, F. K. (2002). An accurate model of wave refraction over shallow water. *Computers & Graphics*, 26(2):291–307.
- Gonzalez, R. C. and Woods, R. E. (1992). *Digital Image Processing*. Addison-Wesley, Reading, MA.
- Mall, H. B. and da Vitoria Lobo, N. (1995). Determining wet surfaces from dry. In *ICCV*, pages 963–968.
- Murase, H. (1992). Surface shape reconstruction of a non-rigid transparent object using refraction and motion. *IEEE Transactions on Pattern Analysis and Machine Intelligence*, 10(10):1045–1052.
- Premoze, S. and Ashikhmin, M. (2001). Rendering natural waters. *Computer Graphics Forum*, 20(4).
- Shefer, R., Malhi, M., and Shenhar, A. (2001). Waves distortion correction using cross correlation. (<http://visl.technion.ac.il/projects/2000maor/>). <http://visl.technion.ac.il/projects/2000maor/>.
- Szeliski, R. and Shum, H.-Y. (1997). Creating full view panoramic image mosaics and environment maps. In *SIGGRAPH '97: Proceedings of the 24th annual conference on Computer graphics and interactive techniques*, pages 251–258, New York, NY, USA. ACM Press/Addison-Wesley Publishing Co.
- Walker, R. E. (1994). *Marine Light Field Statistics*. John Wiley & Sons.
- Wang, Z. and Simoncelli, E. P. (2004). Local phase coherence and the perception of blur. In Thrun, S., Saul, L., and Schölkopf, B., editors, *Advances in Neural Information Processing Systems 16*. MIT Press, Cambridge, MA.
- Young, I. R. (1999). *Wind Generated Ocean Waves*. Elsevier.